Published in final edited form as:

Am J Reprod Immunol. 2019 November ; 82(5): e13181. doi:10.1111/aji.13181.

Intrauterine inhibition of chemokine receptor 4 signaling modulates local and systemic inflammation in ovine pregnancy

Stacia Z McIntosh[1], **Clara J Maxam**[1], **Marlie M Maestas**[1], **Kelsey E Quinn**[1,2], **Ryan L Ashley**[1,*]

[1]Department of Animal and Range Sciences, New Mexico State University, Las Cruces, New Mexico, USA

Abstract

Problem: Chemokines help coordinate inflammation within the fetal-maternal microenvironment during gestation. The chemokine CXCL12 signaling through its receptor CXCR4 regulates inflammatory activity, but this phenomenon is not well understood during pregnancy, and there are no reports exploring the role of this pair in peripheral immune tolerance during gestation. Herein, we hypothesize that intrauterine CXCL12-CXCR4 signaling governs local and systemic immunomodulatory dynamics during early gestation in ewes.

Method of Study: Osmotic pumps were surgically installed for intrauterine infusion of a CXCR4 inhibitor, AMD3100, beginning on day 12 post-breeding in sheep. Endometrial tissues were collected on day 35 of gestation and evaluated for inflammatory potential, Akt pathway activation, and autophagy induction. Demonstrative of peripheral immune activity, levels of select cytokines were assessed in daily blood samples collected throughout the study, as well as in corpus luteum and spleen on day 35.

Results: Anti-inflammatory IL10 was primarily localized to endometrial glandular epithelium with lower abundance when CXCR4 was antagonized. Inhibition of CXCR4 at the fetal-maternal interface resulted in less activation of Akt in endometrium, while evidence of autophagy induction was greater. Corpora lutea from ewes receiving intrauterine AMD3100 exhibited lower interferon gamma (IFNG) expression. Blood inflammatory potential was differentially altered in a temporal fashion throughout infusion. IL10 abundance in spleen was greater following CXCR4 inhibition at the fetal-maternal interface, while IFNG was less.

Conclusion: Intrauterine CXCL12-CXCR4 signaling governs endometrial and systemic inflammation; disruption of this axis may have detrimental impacts on offspring and maternal health.

Keywords

autophagy; corpus luteum maintenance; CXCL12; CXCR4; inflammation mediators; interferon-gamma; interleukin-10

[*]**Correspondence:** Department of Animal and Range Sciences, New Mexico State University, PO Box 30003 MSC 3-I, Las Cruces, NM 88003, ryashley@nmsu.edu.

[2]Currently at Department of Cell Biology and Physiology, University of North Carolina, Chapel Hill, North Carolina, USA

1 | INTRODUCTION

Pregnancy presents a unique physiological phenomenon demonstrated by the presence of a growing semiallogeneic conceptus created by maternal and paternal genomic material. In other instances when the body is invaded by foreign material, it responds with help from the innate and acquired immune systems to recognize and eliminate foreign bodies and/or pathogenic organisms. Such targeted destruction of the conceptus however does not typically occur in normal pregnancy, which has sparked numerous theories regarding the immunological paradox that pregnancy presents. Growing evidence supports the idea of a pro-inflammatory fetal-maternal microenvironment during the first trimester mediated by chemokines and cytokines from fetal trophoblasts.[1]

Chemokines are small, chemotactic cytokines, named such due to their ability to recruit leukocytes, many of which have been linked to implantation and placental development.[2] Namely, trophoblast-derived C-X-C motif chemokine ligand 12 (CXCL12) is a crucial factor that stimulates trophoblast cell survival, migration, and invasion.[3,4] We recently demonstrated that the signaling axis initiated by CXCL12 binding to its receptor, C-X-C motif chemokine receptor 4 (CXCR4), drives placental vascularization. Ovine trophectoderm cells treated with CXCL12 increase angiogenic factor expression[5], and intrauterine inhibition of CXCR4 in vivo negatively impacts ovine placental angiogenesis.[6] In murine models, $CXCR4^+$ dendritic cells aid in vascular expansion of decidua during early pregnancy, and inhibition of CXCR4 decreases recruitment of dendritic cells to the fetal-maternal interface.[7] Still, the primary task of immune cells is that of host defense. Despite multitudinous accounts of CXCL12-CXCR4 signaling regulating leukocyte migration and differentiation both systemically and in endometrium[8–11], the impact of this signaling axis on inflammatory cytokine dynamics in the uterus remains poorly understood.[12]

Similar to the fetal-maternal interface, immune responses are also evident in circulating blood of pregnant women. Peripheral T regulatory $CD4^+CD25^+$ cells are upregulated and activated in normal human pregnancy, while $CD8^+$ cells gain a memory phenotype that persists postpartum.[13,14] CXCR4 may facilitate early pregnancy events by modifying immune cell populations in peripheral blood. Although CXCL12-CXCR4 signaling has immunomodulatory capabilities, reports exploring the role of this pair in peripheral immune tolerance during pregnancy are lacking.

Interferon tau (IFNT), a cytokine from ruminant conceptuses, functions as the primary signal for maternal recognition of pregnancy through various mechanisms including stimulating expression of interferon-stimulated genes (ISG) in peripheral blood leukocytes and signifying activation of the maternal innate immune response.[15] Once believed to act solely within the confines of the uterus, IFNT is now understood to stimulate expression of pregnancy-protective genes in periphery[15] and prolong lifespan of the corpus luteum (CL)[16], the dynamic, crucial source of progesterone. Similar to that demonstrated by IFNT, CXCL12-CXCR4 signaling at the fetal-maternal interface likely initiates an immune response locally as well as in periphery, possibly altering inflammation in the CL and immunomodulatory organs such as the spleen. We hypothesized that intrauterine CXCL12-

CXCR4 signaling governs local and systemic inflammatory potential during early gestation in ewes.

In the present study, we used our ovine model featuring a novel, targeted intrauterine administration of the specific CXCR4 inhibitor, AMD3100.[6] The 14-day infusion period began on day 12 post-breeding and tissues were collected on day 35, which coincides with peak endometrial CXCR4 expression in the pregnant ewe and a well-established placenta.[5,17] We evaluated inflammatory potential and leukocyte phenotype in circulation throughout the infusion period. Upon completion, we analyzed pro-inflammatory cytokines IL12, interferon gamma (IFNG), and tumor necrosis factor (TNF), and anti-inflammatory mediators IL10 and transforming growth factor beta-1 (TGFB1) in endometrium, CL, and spleen. Cellular stability in endometrial samples was also explored by assessing Akt phosphorylation at S473 (Akt pS473), and autophagy induction as demonstrated by abundance of microtubule-associated protein 1 light chain 3 beta (LC3B).

2 | MATERIALS AND METHODS

2.1 | Animals and treatments

All procedures involving animals were approved by the New Mexico State University Institutional Animal Care and Use Committee. To control cyclicity and time breeding, Rambouillet-cross ewes were implanted with intravaginal controlled internal drug release (CIDR) inserts containing progesterone for 5 days. Upon CIDR removal, two 5-mg i.m. injections of dinoprost tromethamine (Lutalyse; Zoetis, Parsippany, NJ, USA) were administered 4 h apart to synchronize estrus. The study used a total of 15 animals. Ewes were mated by a fertile ram and randomly placed into experimental groups of either control (PBS; n = 8) or treatment (AMD3100; n = 7). Osmotic pumps engineered for 5 μL/h delivery over 14 days (catalog number 2ML2; Alzet, Cupertino, CA, USA) were filled with AMD3100 (4120 ng; Selleckchem, Houston, TX, USA) or PBS (137 mM NaCl, 2.7 mM KCl, 10 mM Na_2HPO_4, 1.8 mM KH_2PO_4, pH 7.4; control) according to manufacturer's instructions. On day 12 post-breeding, ewes were anesthetized with a mixture of 5 mg xylazine and 100 mg ketamine (1 mL; i.v.) and maintained on isofluorane throughout surgical procedures as previously described.[6] All ewes received pumps connected to catheters surgically inserted at the uterotubal junction, releasing contents directly into the uterine horn ipsilateral to the CL. Pumps were anchored to the broad ligament with super glue and secured with suture. On day 35 post-breeding, ewes were anesthetized with sodium pentobarbital (20 mg/kg; i.v.) and reproductive tracts removed via mid-ventral laparotomy. Pregnancy was determined by presence of a conceptus and embryonic survival was calculated by dividing the number of concepti by the number of corpora lutea. Neither pregnancy success nor embryonic survival at day 35 were impacted by treatment, and crown-rump length of each conceptus was measured and recorded at tissue collection (Table 1). Ewes determined to be not pregnant at tissue collection (PBS = 3; AMD3100 = 2) were removed from the study. Ewes were euthanized by exsanguination while under anesthesia.

2.2 | Tissue collection

Daily blood samples were collected from days 10 through day 35 of pregnancy via jugular venipuncture into 10 mL EDTA vacutainer tubes and subsequently centrifuged at 4 °C for 30 min at 3750 g. From each tube, plasma and buffy coats were collected for AMD3100 analysis and RNA extraction and stored at −20 °C and −80 °C, respectively. On day 15 of pregnancy, an additional 20 mL of whole blood was collected as described above and immediately subjected to peripheral blood mononuclear cell (PBMC) isolation.

Spleen, CL, and endometrial (caruncle and intercaruncle) tissues were collected at necropsy on gestational day 35 and snap-frozen in liquid nitrogen before storage at −80 °C until further analysis. Raised, aglandular caruncle structures were carefully separated from glandular intercaruncular regions of endometrium at tissue collection, in order to delineate differences specific to the physiologically distinct regions of endometrium. Samples from reproductive tissues were collected from the uterine horn or ovary ipsilateral to pump installation.

2.3 | Ultra-high-performance liquid chromatography (UPLC)

AMD3100 was extracted from ovine plasma with methyl t-butyl ether, followed by back extraction in 0.5% trifluoroacetic acid.[18] A Kinetex® Biphenyl 2.6 μm column (100 X 2.1 mm; Phenomenex, Torrance, CA, USA) was used for reversed phase chromatography with 0.1% formic acid in water for mobile phase A and 0.1% formic acid in methanol for mobile phase B. Flow rate was 0.2 mL/min and injection volume was set to 10 μL. The total runtime was 8.6 min. Figure 1 shows MS/MS spectrum achieved for AMD3100.

2.4 | RNA isolation and quantitative PCR (qPCR)

Total RNA was extracted per manufacturer's instructions using 1 mL Tri-Reagent BD (Molecular Research Center, Cincinnati, OH, USA) supplemented with 30 μL 5 N acetic acid for buffy coats and 1 mL Tri Reagent (Molecular Research Center) per 100 mg of tissue for CL and spleen. All RNA samples were eluted with nuclease-free water. Buffy coat RNA was treated with RNase-free DNase (Qiagen, Venlo, Netherlands) prior to purification with the RNease MinElute Cleanup Kit (Qiagen), while RNA from CL and spleen was treated with DNase using the TURBO DNA-free kit (Thermo Fisher Scientific, Waltham, MA, USA). Quantity and purity of RNA were determined using a NanoDrop-2000 spectrophotometer (Thermo Fisher Scientific), and samples were stored at −80 °C until further analysis. Synthesis of cDNA and qPCR analysis were completed as previously described[5] using primers listed in Table 2. Relative gene expression was graphed with $2^{-\Delta\Delta Cq}$.

2.5 | PBMC isolation

Equal amounts of whole blood were inverted with RPMI-1640 medium with 1% antimycotic/antibiotic (Thermo Fisher Scientific), layered over Histopaque-1077 (catalog number 10771; Sigma-Aldrich, St. Louis, MO, USA), and centrifuged at 500 g for 45 min at room temperature with no brake. PBMC interface from each sample was isolated, diluted to 20 mL with RPMI-1640, and centrifuged at 300 g for 6 min at 4 °C. All steps that follow are at 4 °C unless otherwise noted. Supernatant was removed and replaced with 1

mL RPMI-1640. Two mL red blood cell lysis buffer (0.15 mM NH_4Cl, 10 mM $KHCO_3$, 0.1 mM Na_2EDTA, pH 7.2-7.4) was added and samples were incubated on ice for 3 min until an additional centrifugation at 300 g for 6 min. The remaining PBMC pellet was resuspended in 750 μL PBS supplemented with 2% FCS (flow buffer), counted using a Countess Automated Cell Counter (Thermo Fisher Scientific), and diluted to 10^6 cells/mL with flow buffer.

2.6 | Flow cytometry

Approximately 500,000 cells per sample were acquired for analysis. Cell suspension aliquots of 100 μL were placed in wells of a 96-well v-bottom plate, stained for flow cytometry analysis using either anti-CD8 (catalog number MCA837F; Bio-Rad Laboratories, Hercules, CA, USA) or anti-CD4 (catalog number MCA2213F; Bio-Rad Laboratories) FITC-conjugated antibodies, and subsequently incubated for 45 min. Samples were protected from light for all subsequent steps. Stained cell suspensions were washed by centrifuging the plate at 300 g for 7 min, removing supernatant and resuspending the pellet in additional 100 μL flow buffer, twice. Pellets were resuspended in 150 μL cold PBS, transferred to 1.7 mL microcentrifuge tubes, and 150 μL cold flow fixative (100% ethanol) was added dropwise while vortexing samples vigorously. Within 24 h, cells were resuspended with an additional 200 μL of PBS and analyzed by Accuri C6 (BD Biosciences, San Jose, CA, USA) using BD Accuri C6 Plus (BD Biosciences).

Data were analyzed using FCS Express 4 (De Novo Software, Los Angeles, CA) (Figure 6A and B). Ten thousand events were captured from each sample. A gate was set to distinguish T lymphocytes using forward and side scatter plots, and $CD8^+$ and $CD4^+$ cells were identified within the gated population. Gates used were identical for all samples. An isotype control (catalog number MCA929F; Bio-Rad Laboratories) was used to control for non-specific binding and establish gates to identify cell populations. Cell populations are represented as a percentage of gated events (lymphocytes).

2.7 | Protein isolation and immunoblotting

CL and spleen tissues were homogenized using 1 mL radioimmunoprecipitation assay (50 mM Tris, 2 mM EDTA, 150 mM NaCl, 0.1% SDS, 1.0% Triton X-100) buffer supplemented with phosphatase and protease inhibitor (Roche Applied Sciences) per 100 mg of tissue. Isolates were placed on ice for 15 min, centrifuged at 12,000 g for 10 min at 4 °C and supernatants collected. Protein concentrations were determined by bicinchoninic acid protein assay (Thermo Fisher Scientific) and lysates stored at −80 °C until further analysis.

Equal amounts of protein were separated by SDS-PAGE using 10% polyacrylamide gel under either reducing or non-reducing conditions and transferred to methanol-activated polyvinyl difluoride membranes for immunoblotting. Membranes were blocked in solutions containing either 5% non-fat milk or 5% BSA made in Tris-buffered saline (TBS; 68.4 mM Tris, 10 mM NaCl, pH 7.6) containing 0.10% TWEEN 20 (TBST) for 1 h at room temperature. Blocking solution was then supplemented with a primary antibody specific to either Akt pS473 (1:1000; catalog number 9271L; Cell Signaling Technology, Danvers, MA, USA), IFNG (1:2000; catalog number MCA1964; Bio-Rad Laboratories), IL10 (1:2000; catalog number ab134742; Abcam, Cambridge, UK), or LC3B (1:1000; catalog

number PA1-46286; Thermo Fisher Scientific) and membranes were subsequently incubated overnight at 4 °C. The following day, membranes were washed for 20 min in TBST and incubated with either goat anti-mouse (1:5000; catalog number 1115-035-146; The Jackson Laboratory, Bar Harbor, ME, USA) or goat anti-rabbit (1:4000; catalog number 65-6120; Thermo Fisher Scientific) IgG-horseradish peroxidase-conjugated secondary antibody for 1 h at room temperature. After washing membranes for 20 min, proteins were visualized using the Immun-Star™ WesternC™ kit (Bio-Rad Laboratories) and detected with ChemiDoc™ XRS and Image Lab Software Version 3 (Bio-Rad Laboratories). Equal loading of protein was demonstrated using antibodies for either glyceraldehyde phosphate dehydrogenase (GAPDH; 1:1000; catalog number 3683; Cell Signaling Technology) or total Akt (1:2000; catalog number 9272; Cell Signaling Technology) using incubation conditions noted above.

2.8 | Immunohistochemistry

Immunofluorescence was used for detection and cellular localization of IL10 protein in ovine uterine horn tissue. Paraffin embedded tissue sections underwent deparaffinization using a clearing agent, followed by rehydration washes containing decreasing concentrations of ethanol (100% for 2 X 3 min, 95% for 3 min, 70% for 3 min, and 50% for 3 min). Ethanol was then rinsed off slides for 10 min using cold running tap water. Antigen retrieval was accomplished by boiling samples for 10 min in Tris-EDTA buffer (10 mM Tris, 1 mM EDTA, pH 9.0) followed by a wash with cold, running tap water for 10 min, and an additional 2 X 5 min agitation in wash buffer (68.4 mM Tris, 10 mM NaCl, 0.025% Triton X-100, pH 7.6). Slides were then incubated for 30 min with Image-iT FX signal enhancer (Invitrogen, Eugene, OR, USA), and non-specific binding blocking agent and permeabilization were subsequently combined for a 1-h incubation with TBS containing 0.1% Triton X-100 and 10% normal goat serum. Samples were then incubated with primary antibody specific to IL10 (1:200; catalog number ab134742; Abcam) diluted in TBS supplemented with 1% bovine serum albumin at 4 °C. This technique used a hydrophobic pen barrier to incubate tissue sections with antibody for 16-18 h in a humidified chamber. The next day, slides went through agitated washes for 2 X 5 min, followed by 1-h incubation with a secondary antibody tagged with a fluorescent label (1:200; catalog number A11031; Life Technologies, Eugene, OR, USA). Samples were protected from light for this step and all remaining. Slides were rinsed with TBS 3 X 5 min, mounted using Fluoromount (Thermo Fisher Scientific) containing 4′,6-diamidino-2-phenylindole to counterstain nuclei and preserve tissue, and stored at 4 °C.

Slides were imaged using an Axio Observer.Z1 microscope (Carl Zeiss Microscopy, Oberkochen, Germany) at 20x magnification with identical exposure times for each channel. Images (5−6 per slide) were captured using an Axiocam 506 camera (Carl Zeiss Microscopy) and integrated density value for glandular IL10 was measured using the freehand selection tool in Fiji/Image J (NIH, Bethesda, MD, USA).

2.9 | Statistical analysis

The experimental design was completely randomized, with ewe as the experimental unit. Target gene Cq values were normalized to that of GAPDH for each sample using the ΔCq method[19] and data were analyzed using $2^{-\Delta\Delta Cq}$ values. Chemiluminescent signals for

western blots were evaluated using mean value (intensity) with Image Lab Software (version 4.1; Bio-Rad Laboratories) for each band, which was normalized by dividing mean value for the protein of interest by that of the loading control. Fluorescence integrative density values were normalized by subtracting the background fluorescence of each image from that of glandular IL10.

Pregnancy rates were analyzed by X^2 using Prism (version 8; GraphPad Software Inc., San Diego, CA, USA). Blood cytokine and progesterone levels were analyzed using the mixed procedure of SAS (version 9.4; SAS Institute Inc., Cary, NC, USA) with day post-breeding as a repeated measure. Day, treatment, and day × treatment interactions were included in our model. All other results were analyzed by an unpaired, two-tailed Student's *t*-test using Prism. If the variance significantly differed, Welch's correction was used. All tests were deemed significant if $P \leq 0.05$.

3 | RESULTS

3.1 | Effects of intrauterine CXCR4 inhibition on endometrium and CL inflammation

To evaluate altered local inflammatory potential resulting from CXCR4 inhibition at the fetal-maternal interface, we used a combination of qPCR and immunohistochemistry to assess mRNA expression and protein localization, respectively. Pro-inflammatory *IL12A* expression increased in glandular endometrium (intercaruncular) of ewes receiving local AMD3100 infusion compared to control counterparts, while transcripts for all other cytokines tested were unchanged in endometrial samples, aside from *IFNG*, which was not detected in aglandular (caruncular) tissue (Figure 2A and B). Immunoreactive IL10 was localized mainly to the uterine glandular epithelium with lower abundance ($P < 0.05$) in AMD3100-infused ewes compared to control (Figure 2C, D, and E).

With respect to intracellular signaling, intercaruncle and caruncle tissues were characterized by reduced ($P < 0.05$) Akt signaling as abundance of Akt phosphorylated at S473 was diminished in ewes receiving AMD3100 compared to control (Figure 3A). Opposite to this effect, greater abundance ($P < 0.05$) of LC3B-II, a marker for induction of autophagy, was observed in endometrium from AMD3100-treated ewes compared to controls (Figure 3B).

Inhibiting CXCR4 at the fetal-maternal interface via intrauterine infusion of AMD3100 resulted in altered cytokine gene and protein expression in the CL. *IFNG* mRNA expression in CL was reduced ($P < 0.05$) reciprocated by less IFNG protein ($P < 0.05$) confirmed with western blot (Figure 4) in CL from ewes receiving intrauterine AMD3100 compared to ewes receiving PBS. All other transcripts tested were present, but unchanged with treatment.

3.2 | Effects of intrauterine CXCR4 inhibition on circulating blood cells and spleen inflammation

All inflammatory mediators were detected in RNA from circulating white blood cells across days tested. Compared to control ewes, expression of *CXCR4* in white blood cells transiently increased ($P < 0.05$) on day 16 in ewes when CXCR4 was inhibited at the fetal-maternal interface (Figure 5A). Anti-inflammatory *TGFB1* rose in expression in response to AMD3100 treatment on days 14 ($P < 0.05$), 16 ($P < 0.01$), and 20 ($P < 0.05$) (Figure

5B). Pro-inflammatory cytokine *IL12A* dropped in circulation of AMD3100-treated ewes immediately following pump installation, returned to normal levels, and later exhibited a tendency for increased expression on day 34 ($P < 0.1$) (Figure 5C). Similarly, *IFNG* was temporally elevated on day 35 ($P < 0.01$) (Figure 5D), while *TNF* increased on days 20 ($P < 0.001$) and 22 ($P < 0.01$) in AMD3100-infused ewes compared to control (Figure 5E). Conversely, *IL10* mRNA was transiently reduced in circulation of ewes when CXCR4 was antagonized at the fetal-maternal interface with lower *IL10* on day 30 ($P < 0.01$) and tendency for less on days 24 and 28 ($P < 0.1$) compared to control (Figure 5F).

Flow cytometry was used to determine abundance of cells positive for CD8 and CD4 in circulating blood of pregnant ewes following inhibition of CXCR4 at the fetal-maternal interface. Percentage of $CD8^+$ T lymphocytes decreased ($P < 0.05$) in peripheral blood three days following onset of AMD3100 treatment in utero compared to control (Figure 6C). On the same day of collection, $CD4^+$ populations remained consistent regardless of treatment (Figure 6D).

Inhibition of CXCR4 signaling at the fetal-maternal interface resulted in altered protein abundance for IL10 and IFNG in the spleen. Protein analysis revealed greater abundance ($P < 0.05$) of anti-inflammatory IL10 in ewes receiving AMD3100 (Figure 6E), while IFNG protein abundance was reduced ($P < 0.05$) in spleen compared to control (Figure 6F).

4 | DISCUSSION

Early pregnancy in humans is characterized as an inflammatory event, with spatial and temporal control of inflammatory mediators necessary for endometrial acceptance of the semiallogeneic conceptus. This phenomenon is not well understood in humans and to lesser extent in sheep. However, as ovine pregnancy mirrors human pregnancy in placental development, metabolic functions, and nutrient transport[20], sheep serve as an attractive model for explicating the underlying mechanisms and functions of inflammation during early pregnancy in humans and livestock. One signaling axis likely to mediate localized endometrial inflammation throughout the peri-implantation stage of pregnancy is that initiated by CXCR4, upon binding its ligand CXCL12. Signaling cascades resultant from activation of CXCR4 are implicated in pregnancy viability at the fetal-maternal interface in regard to implantation, angiogenesis, and, namely, cytokine production.[3–5]

We first explored inflammatory characteristics of the endometrium following local inhibition of CXCL12-CXCR4 signaling by AMD3100 infusion. Implantation is characterized by the presence of pro-inflammatory cytokines such as TNF and IFNG facilitating physiologically important events; namely, MUC1 shedding and vascular remodeling, respectively.[21,22] By gestational day 35 in sheep, however, fetal trophoblast cells should be well-adhered to the uterine luminal epithelium and endometrial cell survival gains renewed importance as the fetal-maternal microenvironment transitions into a post-implantation stage. While glandular intercaruncle tissue exhibited greater *IL12A* expression in ewes receiving AMD3100, this effect did not impact IL12 protein abundance (data not shown). However, while AMD3100 infusion had no effect on *IL10* mRNA expression, protein levels for this anti-inflammatory cytokine declined following inhibition of CXCR4. IL10 is widely expressed

on a multitude of both immune and non-immune cell types[23], but imaging data from the current study displays distinct IL10 localization within uterine glandular epithelium of the ovine endometrium.

A potent immunosuppressive cytokine, IL10 is long understood to have implications on fetal-maternal tolerance, with deficiency in IL10 linked to pregnancy pathologies in humans including recurrent spontaneous abortion and preterm birth, as well as preeclampsia.[24,25] IL10 directly activates the Akt signaling axis in other tissues, thereby discouraging autophagy—the regulated process of degrading intracellular proteins and organelles.[26] Akt is a cell survival kinase implicated in maintaining homeostasis of endometrial cells[27], and inhibiting this pathway reduces cellular proliferation, migration, and invasiveness.[28] Thus, a greater understanding of mediators regulating IL10 production is key to addressing potential sources of pregnancy complications. Of note, less IL10 protein was detected in endometrium of AMD3100-infused ewes, and, more precisely, IL10 declined in the uterine glandular epithelium compared to control ewes. In a similar fashion, Akt activation was reduced in endometrium following CXCR4 signaling inhibition. With these data taken together, it's possible that CXCL12-CXCR4 signaling is central to IL10 synthesis and its subsequent downstream functions. Although the experimental design of this study limits our ability to explore this concept mechanistically, future studies in our lab will investigate the direct impact of the CXCL12-CXCR4 axis on IL10 signaling and subsequent Akt activation in endometrial cells.

The concurrent decrease in IL10 and Akt activation, paired with elevated autophagy induction, provides compelling evidence that the CXCL12-CXCR4 axis serves as a governor of endometrial cellular viability and growth. Regulation of autophagy by this chemokine-receptor pair and subsequent Akt signaling has been reported in other tissues.[29] Further, autophagic activity is implicated in ectopic migration and invasion of endometrial stromal cells[30], and others have reported attenuation of autophagic induction in endometriotic lesions by CXCL12-CXCR4 interaction.[31] Taken together, this provides support for involvement in the pathogenesis of endometriosis, a painful condition defined by ectopic growths of endometrium and with infertility as a common outcome.

Underscoring the intimate communication between the uterus and CL to maintain pregnancy, prostaglandin F2 alpha and IFNT synthesized by the endometrium and trophoblast, respectively, leave the uterus to impact CL lifespan in ewes.[16,32] Aside from IFNT, whether other cytokines or chemokines at the fetal-maternal interface influence CL function or lifespan is not well characterized. As the predominant ovarian structure and primary source of progesterone during early pregnancy, we investigated the impact of inhibiting the CXCL12-CXCR4 axis at the fetal-maternal interface has on CL function and inflammatory potential. While mRNA expression of all other cytokines tested remained similar, less *IFNG* transcript was observed in CL following intrauterine CXCR4 inhibition, an effect reflected by decreased IFNG protein abundance as well. The benefit or detriment of this change on luteal function is currently unclear. Although in vitro treatment of luteinized bovine granulosa cells with IFNG inhibits progesterone production in a dose-dependent manner[33], circulating progesterone levels were unaffected by treatment in the current study ($P = 0.68$; Supplemental Figure 1) despite intrauterine AMD3100 infusion and altered CL

IFNG levels. However, growing evidence suggests that pro-inflammatory cytokines play a supportive role in early CL growth.[34,35] IFNG is critical to angiogenesis and vascular remodeling at the implantation site[36], and additionally alters localization of tight junctions in maternal endometrium early in gestation. With this in mind, IFNG may perform similar functions in the CL.[37] Indeed, the CL undergoes a marked increase in vascularization during its developmental stages and endothelial cells of the CL, during pregnancy in particular, experience re-arrangement of cell adhesion proteins and downregulation of tight junctions.[38] Whether IFNG is directly involved in these processes in the CL or if CXCL12-CXCR4 signaling mediates these actions is unknown—future research should explore the relevance of CXCL12-CXCR4 signaling and IFNG production on vascularization and the presence and localization of tight junctions in the CL.

Mechanisms responsible for the precise regulation of the immune system yielding a successful pregnancy are not explicitly understood, and influence of fetal-maternal CXCL12-CXCR4 signaling on immunomodulation of systemic circulation or tissues is not known and as such was an additional objective of the current study. Still, the immunological challenge presented by this phenomenon manifests both locally in the uterus, and in periphery, with fluctuations of leukocyte populations and inflammatory cytokine expression in circulating blood and systemic organs. As such, we examined the systemic expression profile provoked by suppressing CXCR4 signaling in the uterus. Inhibition of CXCR4 signaling at the fetal-maternal interface indeed resulted in temporal dysregulation of each transcript in circulation to varying degree on different days of gestation.

The distinct change in *CXCR4*, *TGFB1*, and *IL12A* following onset of intrauterine treatment infusion raised the question as to whether AMD3100 is eliciting an endocrine effect by traveling into peripheral circulation in addition to acting locally. Utilizing ultra-high-performance liquid chromatography (UPLC), we developed a method of quantifying AMD3100 in circulating plasma with a limit of quantification of 3 ng/μL and ability to detect as low as 1.5 ng/μL. The standard calibration curve used for this purpose is available in supplemental figure 2. AMD3100 was not detected in plasma collected through day 17 of gestation during this study, indicating AMD3100 was not present at measurable levels in circulation of the ewes receiving intrauterine infusion. Taken together, these data imply CXCR4 signaling in the uterus as a governor of peripheral immune response during early pregnancy.

Concurrent with the temporal rise in circulating *CXCR4* expression, transcript for *TGFB1* spiked on days 14 through 16 in ewes receiving intrauterine AMD3100 infusion. Meanwhile, *IL10* experienced an opposing effect later, with a tendency for lower expression on days 24 and 26, continuing toward significantly less expression on day 30 when CXCR4 was inhibited at the fetal-maternal interface. Although delayed, the transient response of elevated *IL12A* and *IFNG* on days 34 and 35, respectively, are consistent with previous reports using AMD3100 to block the interaction of CXCL12 and CXCR4 in other tissues.[39,40] IL12 and IFNG have a synergistic relationship deserving of recognition; as IL12 is capable of inducing IFNG production in leukocytes[41], the possibility exists that the subsequent rise in *IFNG* transcript is a consequence of the change in *IL12A* one day prior. Collectively, our data indicate that antagonizing CXCR4 specifically at the fetal-maternal

interface manifests as altered inflammatory potential of circulating white blood cells. While these data are exciting and underscore the importance of the immune system to pregnancy success, additional studies are needed in rodent and human/primate models to determine if similar responses occur in species with a hemochorial placenta.

Converging with altered inflammatory potential in circulating blood, inhibition of CXCL12-CXCR4 signaling by AMD3100 at the fetal-maternal interface appears to discourage differentiation of lymphocytes from a pro-inflammatory phenotype in periphery. $CD8^+$ T cells are considered cytotoxic pro-inflammatory mediators of anti-viral immunity, but as normal pregnancy is not marked by cytotoxicity, the regulation and functional role of these $CD8^+$ T cells is in question. Fewer peripheral cytotoxic T cells may be indicative of greater activity in the uterus, a possible detriment to developmental progress of the conceptus or placental efficiency. In support, the aforementioned elevation of endometrial autophagic activity demonstrates potential involvement in survival and memory formation of local $CD8^+$ T cells.[42] Human decidua, however, is characterized by 45-75% of the lymphocyte population being $CD8^+$ during the first trimester.[43] Although circumstantial, a distinct pattern presents itself in the current study—lower percentage of $CD8^+$ cells in periphery concurrent with elevated *TGFB1*, which is consistent with a decidedly anti-inflammatory environment. The timeline of these noted changes warrants additional exploration in future studies.

A dynamic organ, the spleen is responsible for not only recycling erythrocytes, but also clearance of blood-borne pathogens. Splenic antigen-presenting cells are capable of priming T lymphocytes; therefore, changes observed in the spleen are indicative of peripheral immunological activity resulting from intrauterine infusion of AMD3100. Protein abundance of IL10 was modified in spleen opposite to transcript changes in blood detected 5 days prior, possibly demonstrative of delayed splenic immune response or lasting consequential cytokine production. This is merely speculative, however, because spleen tissues were solely collected on day 35 of gestation. Evaluation of splenic IFNG production revealed protein abundance also contrary to blood mRNA levels. Because protein is demonstrative of functionality, this information likely has greater biological implications than altered transcript in circulation. It should be mentioned that IFNG activity depends on its interaction with the IFNG receptor, and the IFNG moiety capable of binding its cellular receptor exists as a dimer with a molecular weight of 56 ± 2 kDa, and, further, elicits biological activity as a 72 ± 6 kDa tetramer.[44] Functionally, less IFNG at an apparent molecular weight of 30 kDa in the present study is inconclusive, but IFNG-secreting cells are higher in peripheral blood of pregnant women than non-gravid women.[45] Collectively, these results indicate immunosuppressive activity possibly to the detriment of the mother and/or the developing conceptus as a consequence of blocking intrauterine CXCR4 signaling.

In sum, this study presents compelling evidence that intrauterine CXCL12-CXCR4 signaling is central to initiating downstream events that regulate inflammation locally in the endometrium as well as systemically during early pregnancy. By suppressing intrauterine CXCR4 signaling, this study emphasizes not only the importance of local endometrial activity of the CXCL12-CXCR4 axis, but also its systemic implications to govern pregnancy success. Because aberrations of inflammatory cytokine expression have consequences on

intermediary metabolism[46], effects of suppressed CXCL12-CXCR4 signaling on offspring and maternal health due to altered immune cell phenotype and inflammatory potential in blood and spleen deserve exploration. A greater understanding of how this inflammatory environment is regulated is necessary to develop therapeutics for treatment or prevention of pregnancy complications arising from impaired placental development. Harnessing the actions of CXCL12-CXCR4 signaling may serve as a novel approach to modify the fetal-maternal environment during the window when most pregnancy losses occur and impaired placental development transpires.

Supplementary Material

Refer to Web version on PubMed Central for supplementary material.

Acknowledgments:

This work was supported by the “Partnership for the Advancement of Cancer Research: NMSU/FHCRC”, NCI grant U54 CA132383, the New Mexico Agricultural Experiment Station (AES), Cowboys for Cancer Research Award, and an AES graduate research award. Authors extend thanks to Matthew McIntosh for assistance with statistical analysis and to Dr. Dennis Hallford for progesterone quantification. All authors do not have anything to disclose or any potential sources of conflict of interest.

5 | REFERENCES

1. Mor G, Aldo P, Alvero AB. The unique immunological and microbial aspects of pregnancy. Nat Rev Immunol. 2017;17(8):469–482. [PubMed: 28627518]
2. Salamonsen LA, Hannan NJ, Dimitriadis E. Cytokines and chemokines during human embryo implantation: roles in implantation and early placentation. Semin Reprod Med. 2007;25(6):437–444. [PubMed: 17960528]
3. Jaleel MA, Tsai AC, Sarkar S, Freedman PV, Rubin LP. Stromal cell-derived factor-1 (SDF-1) signalling regulates human placental trophoblast cell survival. Mol Hum Reprod. 2004;10(12):901–909. [PubMed: 15475370]
4. Ren L, Liu YQ, Zhou WH, Zhang YZ. Trophoblast-derived chemokine CXCL12 promotes CXCR4 expression and invasion of human first-trimester decidual stromal cells. Hum Reprod. 2012;27(2):366–374. [PubMed: 22114110]
5. Quinn KE, Ashley AK, Reynolds LP, Grazul-Bilska AT, Ashley RL. Activation of the CXCL12/CXCR4 signaling axis may drive vascularization of the ovine placenta. Domest Anim Endocrinol. 2014;47:11–21. [PubMed: 24486002]
6. Quinn KE, Prosser SZ, Kane KK, Ashley RL. Inhibition of chemokine (C-X-C motif) receptor four (CXCR4) at the fetal-maternal interface during early gestation in sheep: alterations in expression of chemokines, angiogenic factors and their receptors. J Anim Sci. 2017;95(3):1144–11153. [PubMed: 28380526]
7. Barrientos G, Tirado-Gonzalez I, Freitag N, et al. CXCR4(+) dendritic cells promote angiogenesis during embryo implantation in mice. Angiogenesis. 2013;16(2):417–427. [PubMed: 23224220]
8. Tiberio L, Del Prete A, Schioppa T, Sozio F, Bosisio D, Sozzani S. Chemokine and chemotactic signals in dendritic cell migration. Cell Mol Immunol. 2018.
9. Kitamura T, Qian BZ, Pollard JW. Immune cell promotion of metastasis. Nat Rev Immunol. 2015;15(2):73–86. [PubMed: 25614318]
10. Griffith JW, Sokol CL, Luster AD. Chemokines and chemokine receptors: positioning cells for host defense and immunity. Annu Rev Immunol. 2014;32:659–702. [PubMed: 24655300]
11. Sanchez-Martin L, Estecha A, Samaniego R, Sanchez-Ramon S, Vega MA, Sanchez-Mateos P. The chemokine CXCL12 regulates monocyte-macrophage differentiation and RUNX3 expression. Blood. 2011;117(1):88–97. [PubMed: 20930067]

12. Piao HL, Tao Y, Zhu R, et al. The CXCL12/CXCR4 axis is involved in the maintenance of Th2 bias at the maternal/fetal interface in early human pregnancy. Cell Mol Immunol. 2012;9(5):423–430. [PubMed: 22885527]
13. Kieffer TE, Faas MM, Scherjon SA, Prins JR. Pregnancy persistently affects memory T cell populations. J Reprod Immunol. 2017;119:1–8. [PubMed: 27863266]
14. Somerset DA, Zheng Y, Kilby MD, Sansom DM, Drayson MT. Normal human pregnancy is associated with an elevation in the immune suppressive CD25+ CD4+ regulatory T-cell subset. Immunology. 2004;112(1):38–43. [PubMed: 15096182]
15. Gifford CA, Racicot K, Clark DS, et al. Regulation of interferon-stimulated genes in peripheral blood leukocytes in pregnant and bred, nonpregnant dairy cows. J Dairy Sci. 2007;90(1):274–280. [PubMed: 17183095]
16. Bott RC, Ashley RL, Henkes LE, et al. Uterine vein infusion of interferon tau (IFNT) extends luteal life span in ewes. Biol Reprod. 2010;82(4):725–735. [PubMed: 20042537]
17. Ashley RL, Antoniazzi AQ, Anthony RV, Hansen TR. The chemokine receptor CXCR4 and its ligand CXCL12 are activated during implantation and placentation in sheep. Reprod Biol Endocrinol. 2011;9:148. [PubMed: 22053725]
18. Hendrix CW, Flexner C, MacFarland RT, et al. Pharmacokinetics and safety of AMD-3100, a novel antagonist of the CXCR-4 chemokine receptor, in human volunteers. Antimicrob Agents Chemother. 2000;44(6):1667–1673. [PubMed: 10817726]
19. Schmittgen TD, Livak KJ. Analyzing real-time PCR data by the comparative C(T) method. Nat Protoc. 2008;3(6):1101–1108. [PubMed: 18546601]
20. Barry JS, Anthony RV. The pregnant sheep as a model for human pregnancy. Theriogenology. 2008;69(1):55–67. [PubMed: 17976713]
21. Ashkar AA, Di Santo JP, Croy BA. Interferon gamma contributes to initiation of uterine vascular modification, decidual integrity, and uterine natural killer cell maturation during normal murine pregnancy. J Exp Med. 2000;192(2):259–270. [PubMed: 10899912]
22. Thathiah A, Brayman M, Dharmaraj N, Julian JJ, Lagow EL, Carson DD. Tumor necrosis factor alpha stimulates MUC1 synthesis and ectodomain release in a human uterine epithelial cell line. Endocrinology. 2004;145(9):4192–4203. [PubMed: 15142990]
23. Cheng SB, Sharma S. Interleukin-10: a pleiotropic regulator in pregnancy. Am J Reprod Immunol. 2015;73(6):487–500. [PubMed: 25269386]
24. Hanna N, Bonifacio L, Weinberger B, et al. Evidence for interleukin-10-mediated inhibition of cyclo- oxygenase-2 expression and prostaglandin production in preterm human placenta. Am J Reprod Immunol. 2006;55(1):19–27. [PubMed: 16364008]
25. Hennessy A, Pilmore HL, Simmons LA, Painter DM. A deficiency of placental IL10 in preeclampsia. J Immunol. 1999;163(6):3491–3495. [PubMed: 10477622]
26. Shi J, Wang H, Guan H, et al. IL10 inhibits starvation-induced autophagy in hypertrophic scar fibroblasts via cross talk between the IL10-IL10R-STAT3 and IL10-AKT-mTOR pathways. Cell Death Dis. 2016;7:e2133. [PubMed: 26962683]
27. Costa AF, Gomes SZ, Lorenzon-Ojea AR, et al. Macrophage migration inhibitory factor induces phosphorylation of Mdm2 mediated by phosphatidylinositol 3-kinase/Akt kinase: Role of this pathway in decidual cell survival. Placenta. 2016;41:27–38. [PubMed: 27208405]
28. Mecca C, Giambanco I, Bruscoli S, et al. PP242 Counteracts Glioblastoma Cell Proliferation, Migration, Invasiveness and Stemness Properties by Inhibiting mTORC2/AKT. Front Cell Neurosci. 2018;12:99. [PubMed: 29692710]
29. Hashimoto I, Koizumi K, Tatematsu M, et al. Blocking on the CXCR4/mTOR signalling pathway induces the anti-metastatic properties and autophagic cell death in peritoneal disseminated gastric cancer cells. Eur J Cancer. 2008;44(7):1022–1029. [PubMed: 18375114]
30. Liu H, Zhang Z, Xiong W, et al. Hypoxia-inducible factor-1alpha promotes endometrial stromal cells migration and invasion by upregulating autophagy in endometriosis. Reproduction. 2017;153(6):809–820. [PubMed: 28348069]
31. Mei J, Zhu XY, Jin LP, Duan ZL, Li DJ, Li MQ. Estrogen promotes the survival of human secretory phase endometrial stromal cells via CXCL12/CXCR4 up-regulation-mediated autophagy inhibition. Hum Reprod. 2015;30(7):1677–1689. [PubMed: 25976655]

32. Thatcher WW, Bartol FF, Knickerbocker JJ, et al. Maternal recognition of pregnancy in cattle. J Dairy Sci. 1984;67(11):2797–2811. [PubMed: 6084020]
33. Best CL, Griffin PM, Hill JA. Interferon gamma inhibits luteinized human granulosa cell steroid production in vitro. Am J Obstet Gynecol. 1995;172(5):1505–1510. [PubMed: 7755064]
34. Brannstrom M, Norman RJ. Involvement of leukocytes and cytokines in the ovulatory process and corpus luteum function. Hum Reprod. 1993;8(10):1762–1775. [PubMed: 8300842]
35. Galvao AM, Ferreira-Dias G, Skarzynski DJ. Cytokines and angiogenesis in the corpus luteum. Mediators Inflamm. 2013;2013:420186. [PubMed: 23840095]
36. Murphy SP, Tayade C, Ashkar AA, Hatta K, Zhang J, Croy BA. Interferon gamma in successful pregnancies. Biol Reprod. 2009;80(5):848–859. [PubMed: 19164174]
37. Cencic A, Guillomot M, Koren S, La Bonnardiere C. Trophoblastic interferons: do they modulate uterine cellular markers at the time of conceptus attachment in the pig? Placenta. 2003;24(8–9):862–869. [PubMed: 13129683]
38. Herr D, Bekes I, Wulff C. Regulation of Endothelial Permeability in the Corpus Luteum: A Review of the Literature. Geburtshilfe Frauenheilkd. 2013;73(11):1107–1111. [PubMed: 24771896]
39. Lukacs NW, Berlin A, Schols D, Skerlj RT, Bridger GJ. AMD3100, a CxCR4 antagonist, attenuates allergic lung inflammation and airway hyperreactivity. Am J Pathol. 2002;160(4):1353–1360. [PubMed: 11943720]
40. Santagata S, Napolitano M, D'Alterio C, et al. Targeting CXCR4 reverts the suppressive activity of T-regulatory cells in renal cancer. Oncotarget. 2017;8(44):77110–77120. [PubMed: 29100374]
41. Ahn HJ, Maruo S, Tomura M, et al. A mechanism underlying synergy between IL12 and IFN-gamma-inducing factor in enhanced production of IFN-gamma. J Immunol. 1997;159(5):2125–2131. [PubMed: 9278298]
42. Xu X, Araki K, Li S, et al. Autophagy is essential for effector CD8(+) T cell survival and memory formation. Nat Immunol. 2014;15(12):1152–1161. [PubMed: 25362489]
43. Erlebacher A Immunology of the maternal-fetal interface. Annu Rev Immunol. 2013;31:387–411. [PubMed: 23298207]
44. Langer JA, Rashidbaigi A, Garotta G, Kempner E. Radiation inactivation of human gamma-interferon: cellular activation requires two dimers. Proc Natl Acad Sci U S A. 1994;91(13):5818–5822. [PubMed: 8016072]
45. Matthiesen L, Ekerfelt C, Berg G, Ernerudh J. Increased numbers of circulating interferon-gamma- and interleukin-4-secreting cells during normal pregnancy. Am J Reprod Immunol. 1998;39(6):362–367. [PubMed: 9645266]
46. Gifford CA, Holland BP, Mills RL, et al. Growth and Development Symposium: Impacts of inflammation on cattle growth and carcass merit. J Anim Sci. 2012;90(5):1438–1451. [PubMed: 22573836]

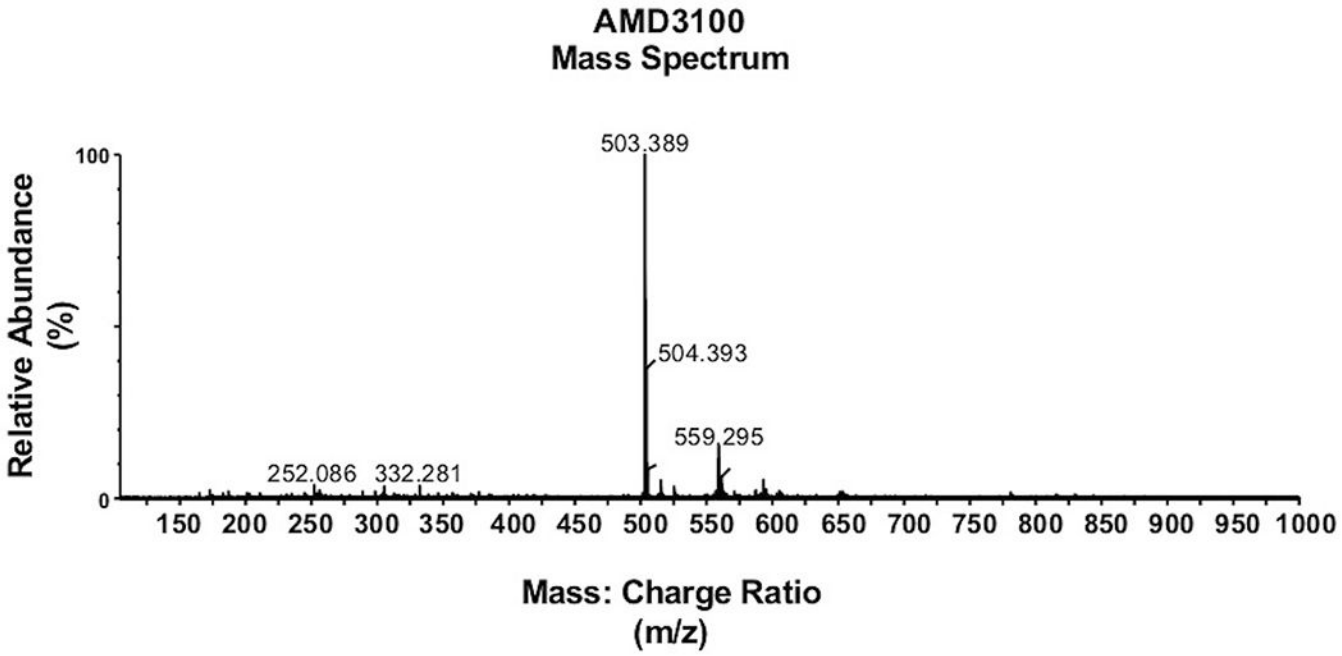

FIGURE 1.

Detection of AMD3100. MS/MS spectrum of AMD3100 standard used to determine calibration curve.

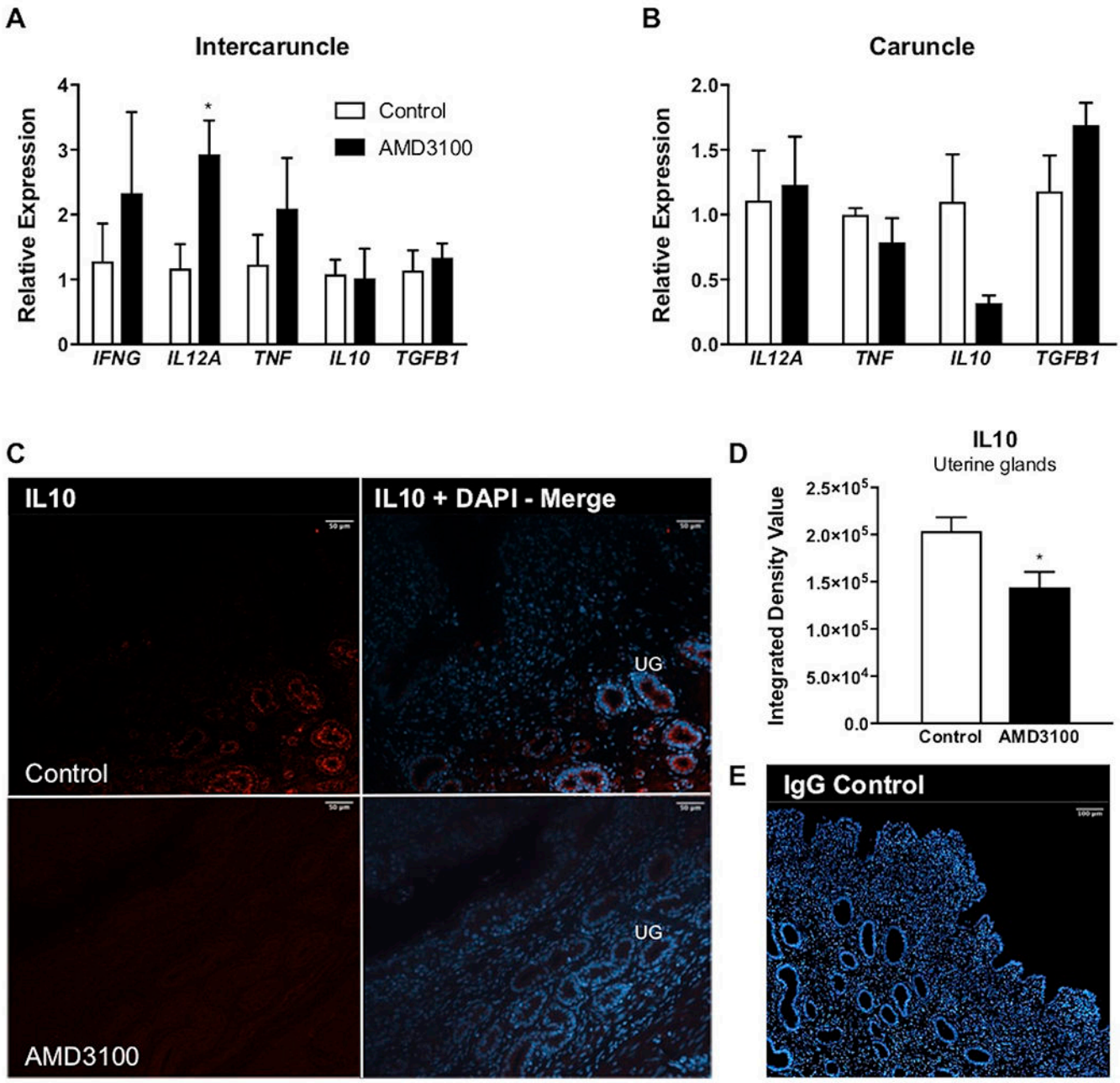

FIGURE 2.

Inflammatory potential following local intrauterine AMD3100 infusion. Relative expression of select inflammatory mediators in intercaruncle (A) and caruncle (B) tissue on day 35 of gestation. Representative 20x magnification images of IL10 (red) localization to uterine glands (UG) in control and AMD3100-infused animals (C), followed by quantification of IL10 integrated density value (D), and representative serum control shown at 10x magnification (E). mRNA data are represented by graphing $2^{-\Delta\Delta Cq}$ and graphs represent the mean ± SEM. Analysis by Student's *t*-test; significance determined at $P < 0.05$ (*).

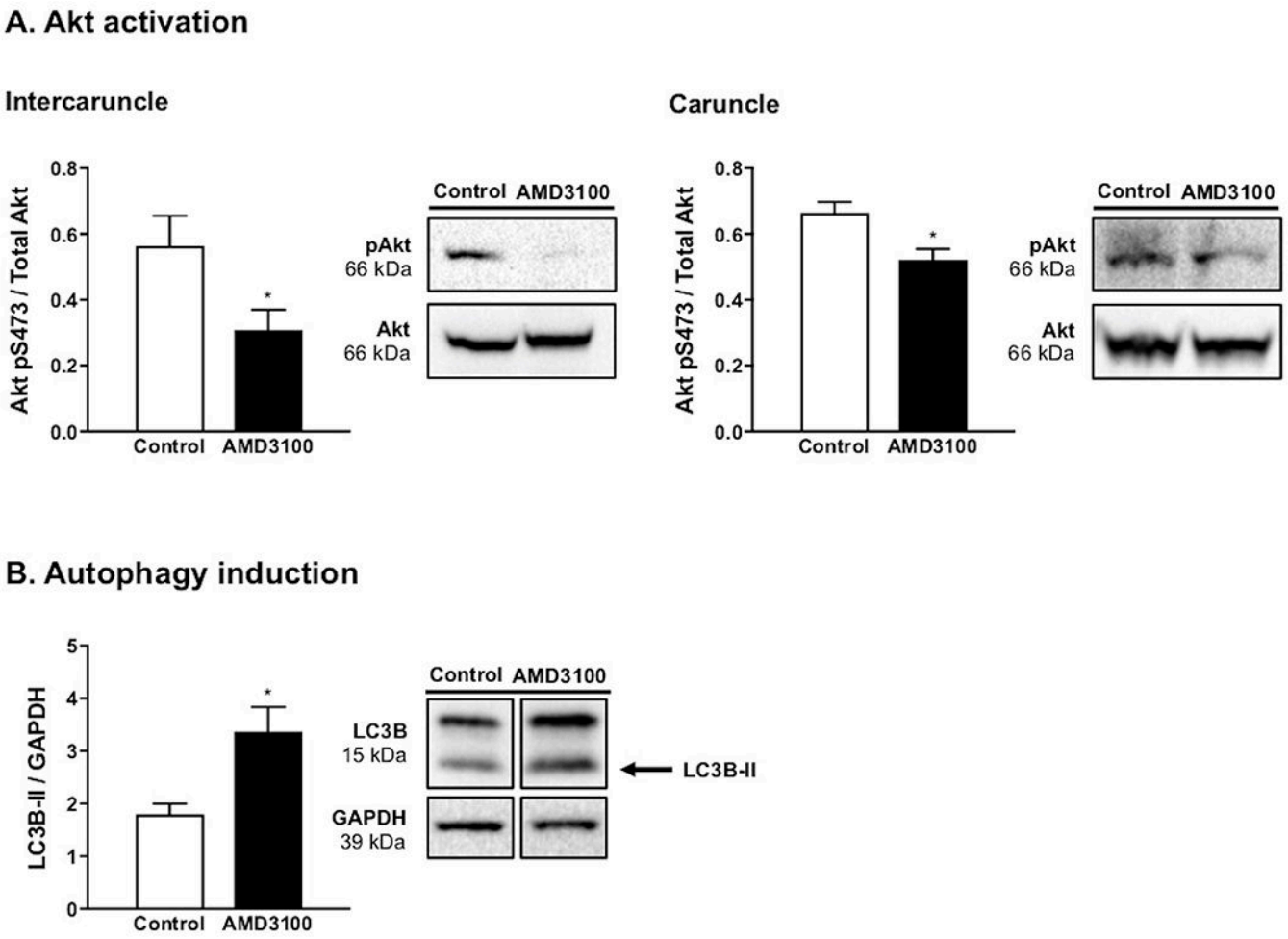

FIGURE 3.

Akt activation and autophagy induction on day 35 of pregnancy following local intrauterine AMD3100 infusion. Akt (S473) activation in intercaruncle and caruncle tissue (A). Endometrial autophagy induction, as demonstrated by quantification of LC3B-II abundance (B). Each graph represents the mean ± SEM and is followed by representative immunoblot. Analysis by Student's *t*-test; significance determined at $P < 0.05$ (*).

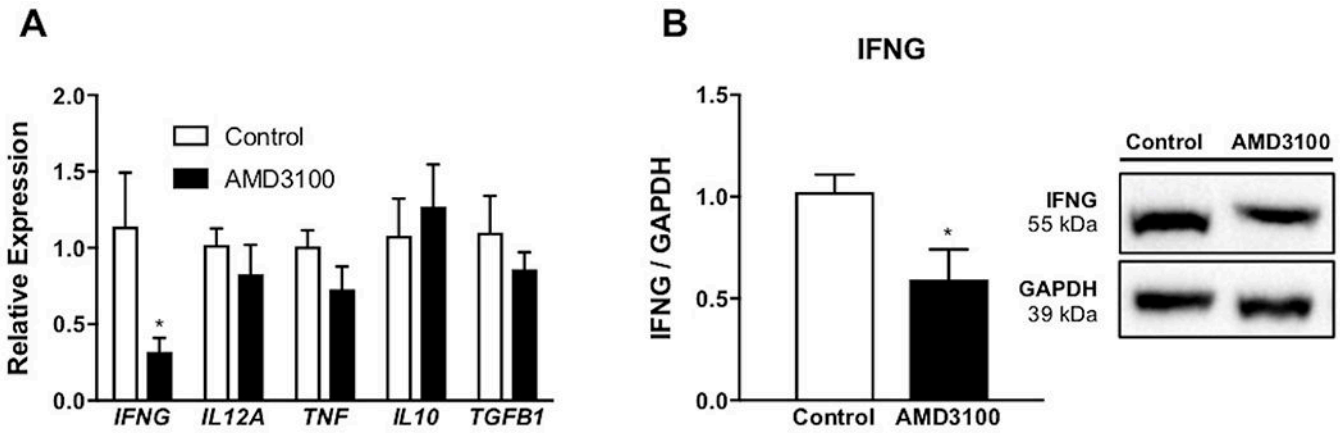

FIGURE 4.

Inflammatory potential in corpora lutea following intrauterine AMD3100 infusion. Relative expression of select inflammatory mediators (A) on day 35 of pregnancy. Protein abundance of IFNG, followed by representative immunoblot (B). mRNA data are represented by graphing $2^{-\Delta\Delta Cq}$ and graphs represent the mean ± SEM. Analysis by Student's *t*-test; significance determined at $P < 0.05$ (*).

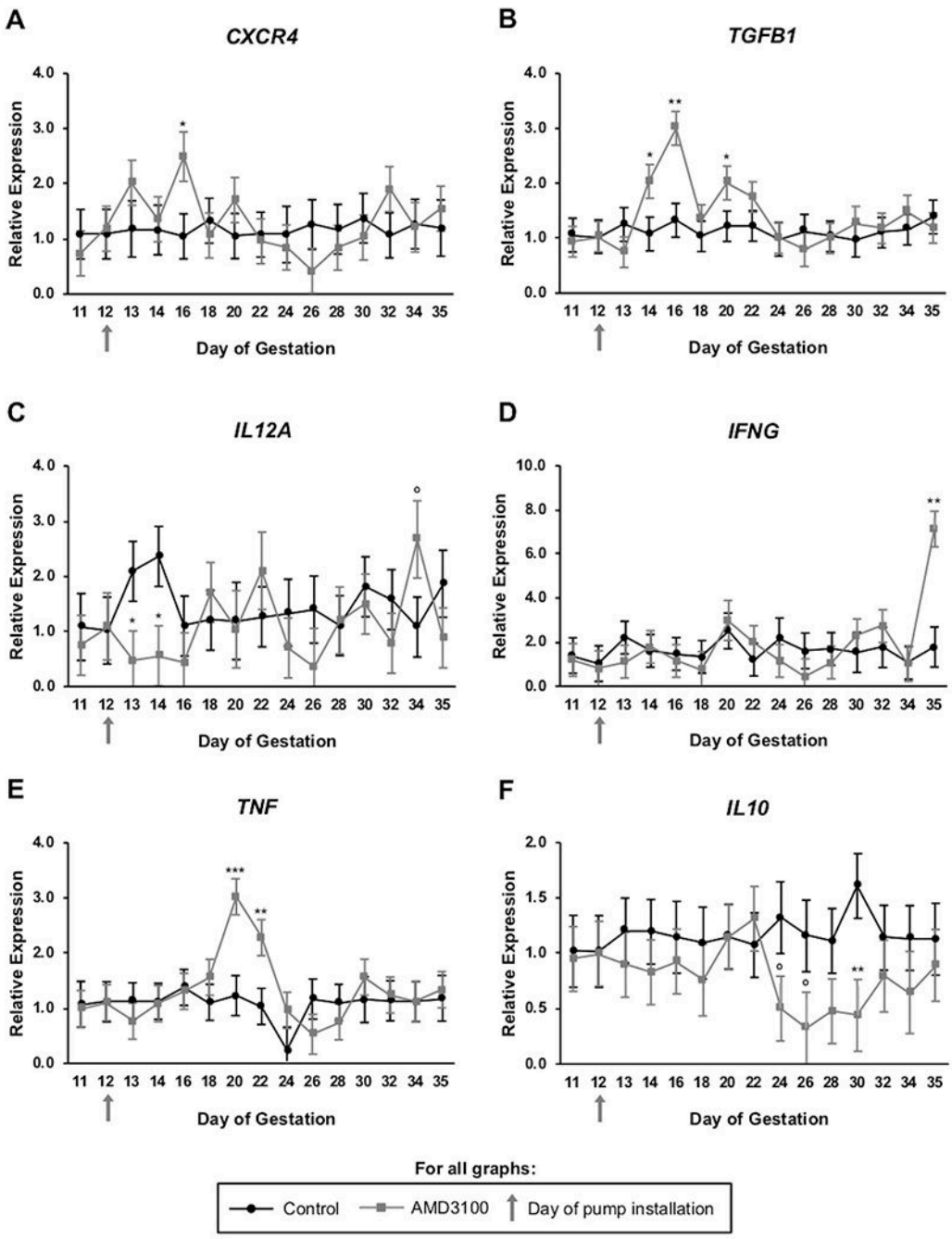

FIGURE 5.

Inflammatory potential of circulating immune cells in pregnant ewes following AMD3100 infusion at the fetal-maternal interface. Graphs for *CXCR4* (A), *TGFB1* (B), *IL12A* (C), *IFNG* (D), *TNF* (E), and *IL10* (F) all represent expression across days 11 through 35 of gestation. mRNA data are represented by graphing $2^{-\Delta\Delta Cq}$ and graphs represent means for each day. Significance determined at $P < 0.05$ (*), $P < 0.01$ (**), $P < 0.001$ (***), and tendency accepted at $P < 0.1$ (°).

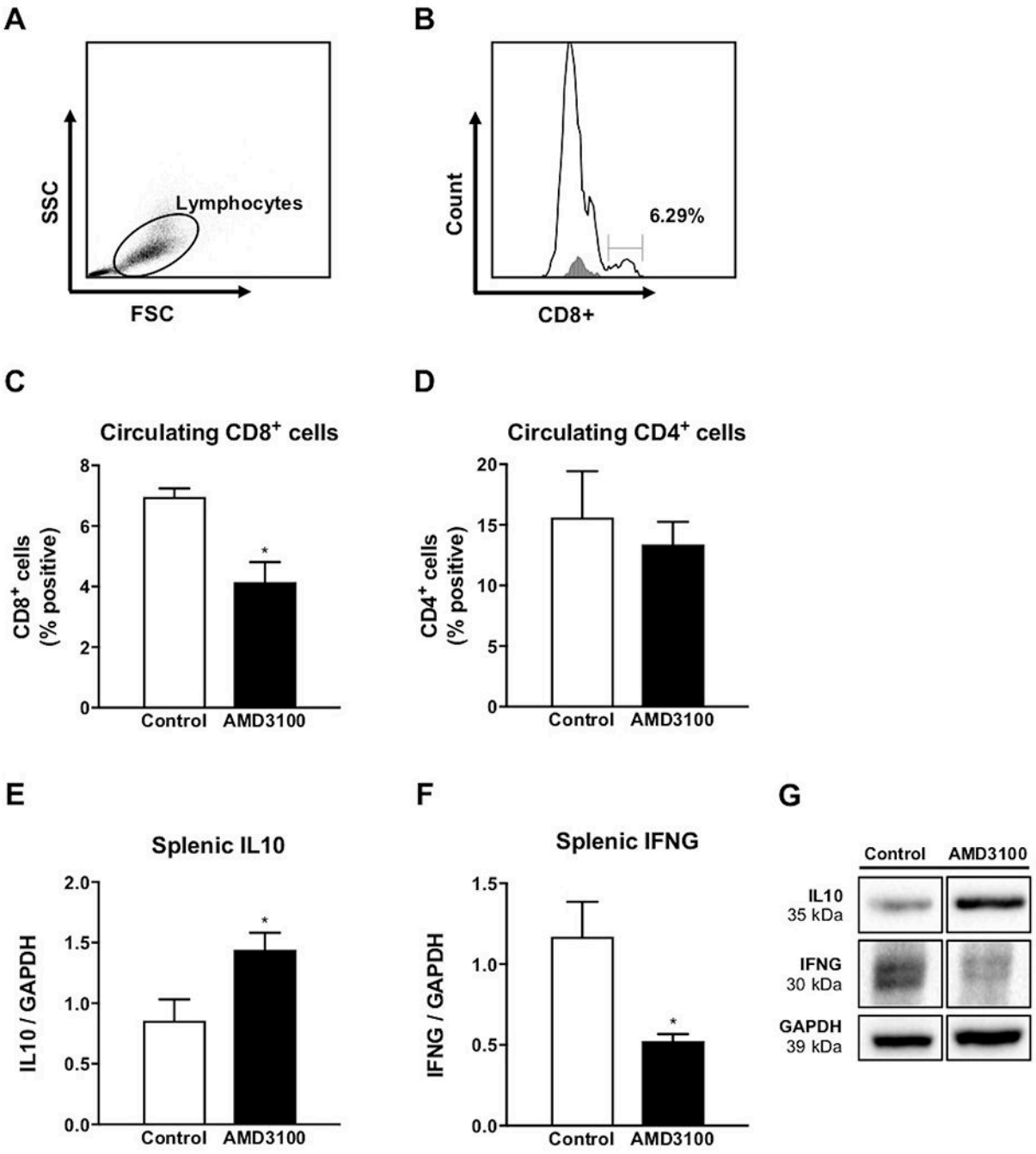

FIGURE 6.

Circulating $CD8^+$ and $CD4^+$ cells on day 15 of gestation following intrauterine AMD3100 infusion. Representative example of a gate set to include lymphocytes using forward and side scatter (FSC/SSC) parameters (A), followed by identification and quantification of $CD8^+$ cells (B). Proportion of cells positive for CD8 (C) and CD4 (D) in ewes receiving AMD3100 compared to control. Splenic cytokine abundance following intrauterine AMD3100 infusion. Protein abundance for IL10 (E) and IFNG (F) on day 35 of pregnancy,

followed by representative immunoblot (G). Graphs represent the mean ± SEM. Analysis by Student's *t*-test; significance determined at $P < 0.05$ (*).

TABLE 1

Pregnancy rate and conceptus data.

	Treatment	
Item	**Control**[1]	**AMD3100**[2]
Pregnancy rate, %	62.50	71.43
Embryonic survival, %	37.50 ± 13	64.29 + 17
Conceptus crown-rump length, cm[3]	1.8 ± 0.12	2.17 ± 0.13 [°]

[1] Four singleton and 2 twin concepti from ewes receiving PBS (control) infusion.

[2] Four singleton and 2 twin concepti from ewes receiving AMD3100 infusion.

[3] For statistical analysis, twin conceptus measurements were averaged.

[°] Tendency accepted at $P < 0.1$.

TABLE 2

Primer sequences for each ovine gene of interest.

Target	Sequence	Accession no.
GAPDH	5'-TGACCCCTTCATTGACCTTC-3' 5'-CGTTCTCTGCCTTGACTGTG-3'	NM_001190390
IL10	5'-GGCGCTGTCATCGTTTTCTG-3' 5'-ACACCCCTCTCTTGGAGCAT-3'	NM_001009327.1
IL12A	5'AGCCACGAATGAGAGTTGCC-3' 5'-TCCAGAAGACAGACAATGCCC-3'	NM_001009736.1
IFNG	5'-GGCTGATTCAAATTCCGGTGG-3' 5'-TCTCCGGCCTCGAAAGAGAT-3'	NM_001009803.1
TNF	5'-GTAGCCCACGTTGTAGCCAA-3' 5'-TCAGGTAAAGCCCGTCAGTG-3'	NM_001024860.1
TGFB1	5'-AGAAGGCTTTCGCCTCAGTG-3' 5'-CCGGAACTGAACCCGTTGAT-3'	NM_001009400.1